Sequence-Controlled Multiblock Copolymers via RAFT Polymerization: Modeling and Simulations[a]

Per B. Zetterlund,* Guillaume Gody, Sébastien Perrier

The synthesis of high-order multiblock copolymers by one-pot sequential monomer addition RAFT polymerization is examined by use of modeling and simulations using PREDICI. The system is the previously experimentally investigated model multiblock homopolymer system comprising 10 blocks of *N,N*-dimethyl acrylamide with average degree of polymerization 10 for each block. The simulations show that despite 10 chain extensions to full conversion, the number of dead chains at the end of the process is only ≈7%. The number fraction of dead chains is known from the number of chains generated from the initiator, and the conditions can thus be tailored with regards to the livingness required.

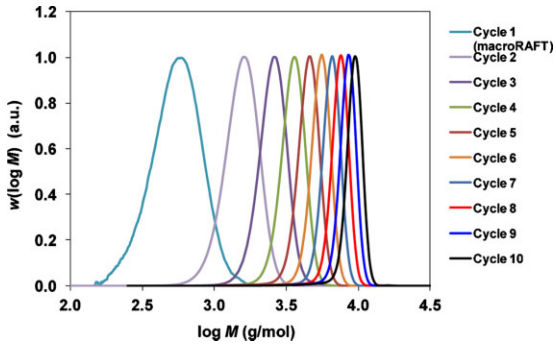

1. Introduction

One of the primary long-standing goals in polymer chemistry is the ability to synthesize (co)polymers with perfect tailor-made structures in terms of molecular weight (MW), MW distribution, monomer sequence distribution, end functionality, and tacticity.[1–5] The microstructure of natural polymers such as proteins and enzymes are "perfect;" the ordering of monomers along the (co)polymer chain as well as the spatial arrangement of functional groups are what enable these macromolecules to perform very specific functions in nature. The tertiary structure of proteins is highly dependent on the exact microstructure of the polymer, and this tertiary structure is instrumental in determining the properties and functions of a protein. The advent of controlled/living radical polymerization (LRP)[6,7] has had an enormous impact on the field of polymer chemistry as well as more applied disciplines such as materials science and nanomedicine. It is now possible to synthesize a wide range of complex macromolecular architectures of well-defined MW by free radical means, e.g., block copolymers, star polymers, etc. However, it remains a difficult challenge to manipulate single chains and control the precise order of monomer units along the chain. Recent progress with regards to regulation of monomer sequences have been made via various approaches, including the use of low MW templates that anchors three monomer units in a specific sequence,[8] selective radical additions of monomers using template initiators with recognition moieties,[9] and approaches based on single addition of a monomer with low tendency toward homopolymerization,[10,11] and a DNA-templated approach.[12] A recent biomimetic approach based on templated radical polymerization in nanoreactors also

Prof. P. B. Zetterlund
Centre for Advanced Macromolecular Design (CAMD), School of Chemical Engineering, The University of New South Wales, Sydney, NSW 2052, Australia
E-mail: p.zetterlund@unsw.edu.au
Dr. G. Gody, Prof. S. Perrier
Department of Chemistry, University of Warwick, Coventry CV4 7AL, UK

[a]**Supporting Information** is available from the Wiley Online Library or from the author.

DOI: 10.1002/mats.201300165

has potential with regards to manipulation of single chains.[13]

Multiblock copolymers represent a class of polymers with controlled monomer sequence distribution, where each individual block can vary significantly in degree of polymerization.[14] Such macromolecular structures have traditionally been limited to relatively few blocks,[15–18] but recent developments have enabled synthesis of highly complex high-order multiblock copolymers, and these approaches now represent convenient and powerful routes toward sequence control. The breakthrough with regards to multiblock copolymer synthesis by LRP was the realization that the high livingness in Cu(0)-mediated radical polymerization makes it possible to conduct iterative polymerizations whereby the polymerization is taken to full conversion in each step followed by addition of the "next" monomer, without intermediate purification steps.[19–25] We have very recently developed methodology based on RAFT polymerization for synthesis of very complex high-order multiblock copolymers using a similar concept based on iterative monomer additions, and essentially full conversion in each step, without intermediate purification.[1,26] This approach enabled us to prepare an icosablock (20 blocks) copolymer with very good control over the MW distribution, as well as a range of other functional multiblock copolymers.[26] This RAFT methodology, which is indeed also applicable to other systems operating via a degenerative transfer mechanism, is based on careful selection of experimental conditions whereby the initiator concentration is minimized relative to the concentration of RAFT end groups while maintaining a sufficiently high polymerization rate. This realization has widely expanded the scope of the RAFT technique with regards to synthesis of complex macromolecular structures, generating sequence-controlled polymers previously not believed to be accessible.

In this work, we have employed the software PREDICI[27] to conduct modeling and simulations to examine and verify the kinetic/mechanistic aspects underlying the success of our recently reported experimental work on RAFT high-order multiblock copolymer synthesis.[1,26] It is confirmed that such complex macromolecular structures are readily accessible via RAFT polymerization provided that the cumulative concentration of radicals generated from the radical initiator is sufficiently low relative to the RAFT agent concentration.

2. Model Description

The system of interest was the iterative homopolymerizations (10 cycles) of *N*,*N*-dimethyl acrylamide (DMA) in dioxane at 65 °C using 2-propanoic acid butyl trithiocarbonate (PABTC) as RAFT agent and azobisisobutyronitrile (AIBN) as initiator. This is the system that we reported a recent experimental study on[1]–the reason for creating a "homopolymer multiblock structure" is that it is a useful model system for more complex systems comprising various different monomer types.

The task at hand is to model ten consecutive RAFT polymerizations, referred to as Cycles 1–10. The first cycle makes use of the low MW RAFT agent PABTC, whereas the corresponding nine cycles involve a macroRAFT agent formed in situ during Cycle 1. The first cycle is inherently more complex than the subsequent cycles because it involves both the pre-equilibrium (low MW RAFT agent) and the core-equilibrium (macroRAFT).[28] In order to make the modeling more tractable, so as to avoid a situation where the model output of Cycle 1 (and hence the output of all subsequent cycles) depends strongly on various assumptions related to rate coefficients and mechanism, it was deemed sensible to start the simulations from Cycle 2. An experimental molecular weight distribution (MWD) of Cycle 1 (taken from our recently published[1] experimental study on RAFT multiblock copolymers, that forms the basis of the present modeling study) was used as model input for Cycle 2. It was thus assumed that the MWD obtained experimentally from Cycle 1 comprised macroRAFT agent of 100% livingness (i.e., all chains have a RAFT ω-end group). Theory (based on the number of chains generated from the initiator during the polymerization) predicts that the livingness after Cycle 1 is 99.4%,[1] and as such the adopted approach appears reasonable.

RAFT polymerization was modeled based on the fundamental RAFT mechanism originally proposed by CSIRO,[29] according to which intermediate radicals do not participate in any reactions other than fragmentation. The fundamental mechanism of RAFT polymerization is well established,[30–32] although the exact fate of the intermediate radicals (their rate of fragmentation and ability to undergo cross-termination reactions and/or other side reactions) remains under debate.[28,33–37] The model, implemented in PREDICI,[27] comprises the reaction steps listed below, where I is initiator, $R^\bullet$ is a low MW initiator radical, M is monomer, $P^\bullet$ is a propagating radical, $Q^\bullet$ is an intermediate radical, D is polymer with a RAFT end group (dormant chain), S is dead polymer, and the subscripts *m* and *n* denote degrees of polymerization. The RAFT agent is a polymeric RAFT agent (Cycle 1 is not modeled; simulations commence from Cycle 2, in which case only polymeric RAFT agent exists – see above), and as such the RAFT pre-equilibrium (involving low MW RAFT agent) need not be considered. Addition of $R^\bullet$ to D followed by fragmentation, which would generate a low MW RAFT agent in situ, was not included in the model ($R^\bullet$ adds to M to generate $P^\bullet$). Given the high ratio of RAFT agent to initiator (>100), the

presence of a very low concentration of such low MW RAFT agent is deemed kinetically insignificant. Termination was assumed to occur via disproportionation only (simulations with 100% termination by combination resulted in a prominent high MW peak (higher MW than main peak) that was not observed experimentally[1]).

$$I \xrightarrow{k_d} 2R^{\bullet} \quad \text{Initiator decomposition} \tag{1}$$

$$R^{\bullet} + M \xrightarrow{k_i} P_1^{\bullet} \quad \text{Initiation} \tag{2}$$

$$P_n^{\bullet} + M \xrightarrow{k_p} P_{n+1}^{\bullet} \quad \text{Propagation} \tag{3}$$

$$P_n^{\bullet} + D_m \xrightarrow{k_{add}} Q_{n+m}^{\bullet} \quad \text{Addition to RAFT end group} \tag{4}$$

$$Q_{n+m}^{\bullet} \xrightarrow{k_\beta} P_m^{\bullet} + D_n \quad \text{Fragmentation} \tag{5}$$

$$P_n^{\bullet} + P_m^{\bullet} \xrightarrow{k_t} S_n + S_m \quad \text{Termination (disproportionation)} \tag{6}$$

It is challenging to model the RAFT fragmentation step, because the model must distinguish between and "remember" the chain lengths of the two polymer chains attached to the central RAFT moiety of the intermediate radical $Q^{\bullet}$. This was accomplished by introducing the fictitious species X and Y based on an earlier developed approach:[38–40]

$$P_n \bullet + D_m \xrightarrow{k_{add}} X_n + Y_m \tag{7}$$

$$X_n \xrightarrow{k_\beta} D_n \tag{8}$$

$$Y_m \xrightarrow{k_\beta} P_m \bullet \tag{9}$$

Fragmentation of adduct radicals was assumed to occur in the "forward" direction only. As such, the overall rate of exchange predicted by the model represents the net (observed) rate of exchange, which is also what experimental values of C_{ex} ($=k_{add}/k_p$) represent in the case of homopolymerization. The fragmentation rate was assumed to be sufficiently fast so as not to be a rate-determining step, following the fundamental RAFT mechanism originally proposed by CSIRO[29] ($k_\beta = 100\ s^{-1}$ in all simulations). The rate of initiation is controlled by the rate of initiator decomposition, and hence the value of k_i has no effect on the simulation (as long as it is not unreasonably low; $k_i = 10^4\ M^{-1}\ s^{-1}$ in the present simulations).

Values of k_p for DMA under the present conditions (dioxane at 65 °C) have not been reported. Based on literature values of k_p for similar monomers ($k_p = 1.28 \times 10^5\ M^{-1} s^{-1}$ for acrylamide in water at 65 °C,[41] $k_p = 1 \times 10^4$–$7 \times 10^4\ M^{-1}\ s^{-1}$ (apparent values due to problems with consistency criteria in pulsed-laser polymerization method) for *N*-isopropyl acrylamide in water at 10 °C[42]), the simulations were conducted with $k_p = 1.7 \times 10^4\ M^{-1} s^{-1}$. This value was arrived at based on preliminary simulations showing that full conversion was reached within each iterative cycle well before the end of the cycle time using this value of k_p. Conversion-dependence and chain-length dependence of k_p were not included in the model. The rate coefficient for decomposition of AIBN at 65 °C: $k_d = 1.925 \times 10^{-5}\ s^{-1}$.[43]

The value of C_{ex} ($=k_{add}/k_p$) was approximated with that reported for *n*-butyl acrylate with the trithiocarbonate macroRAFT agent where the R-group is poly(*n*-butyl acrylate) with a Z-group of SC_4H_9 (i.e., the polymeric version corresponding to PABTC) at 70 °C; $C_{ex} = 34.5$.[44,45] Based on $k_p = 1.7 \times 10^4\ M^{-1} s^{-1}$, it follows that $k_{add} = 5.87 \times 10^5\ M^{-1}\ s^{-1}$. The pre-equilibrium was thus not modeled (only relevant for Cycle 1), which is consistent with the approach adopted whereby the simulations started from Cycle 2, treating the MWD after the first cycle as a macroRAFT agent with 100% livingness (purity).

Chain-length dependence of k_t was accounted for according to the composite model:[46,47]

$$k_t^{i,i} = \begin{cases} k_t^{1,1} \times i^{-\alpha_S} & (i \le i_c) \\ k_t^{1,1} \times 100^{-\alpha_S+\alpha_L} \times i^{-\alpha_L} & (i > i_c) \end{cases} \tag{10}$$

where i is the degree of polymerization of a terminating propagating radical, $k_t^{i,i}$ is the termination rate coefficient between two propagating radicals of degrees of polymerization i, α_S and α_L correspond to "short" and "long" chains, and i_c is the critical degree of polymerization at which the extent of chain-length dependence of k_t changes. The cross-termination rate coefficients were obtained based on the geometric mean model:[47]

$$k_t^{i,j} = (k_t^{i,i} k_t^{j,j})^{0.5} \tag{11}$$

There are currently no relevant experimental data available on chain-length dependent k_t values for DMA. As an approximation, it was deemed reasonable to use parameters pertaining to the composite model as reported for butyl acrylate at 60 °C[48]: $k_t^{1,1} = 2.34 \times 10^9\ M^{-1}\ s^{-1}$; $\alpha_S = 1.21$; $\alpha_L = 0.09$; $i_c = 40$. The above model approximately captures the dependence of k_t on both conversion and propagating radical chain-length (the propagating radical chain length increases with conversion in LRP), although it must of course be stressed that additional error is introduced due to (i) differences in recipes (between the reported butyl acrylate data and the present work), i.e., the k_t versus conversion also depend on polymer concentration, and (ii) different solvents (DMA in dioxane vs. bulk (butyl acrylate)).

Each cycle has to be modeled in PREDICI as a discrete step. It is not possible to "add" monomer, solvent, and initiator at the end of each cycle and simply continue the simulation (as is done in reality in the lab). As such, the approach taken was to (i) use the living polymer from Cycle x as macroRAFT agent in Cycle $x+1$, and (ii) to keep track of the amount (and MWD) of dead polymer formed in each cycle, and subsequently add the cumulative amount of dead polymer formed throughout Cycles 2 to x when constructing the simulated cumulative MWD of dead polymer present after Cycle x. As evident from the equations above, the model does not distinguish between propagating radicals with different α-end groups, i.e., chains with an initiator fragment at the α-end (initiator-derived chains) and chains with a RAFT R-group at the α-end are lumped together as P$^\bullet$. However, it is important to note that all initiator-derived chains are accounted for with regards to the overall number of chains. The initial concentrations of monomer, initiator, and macroRAFT corresponding to each cycle (Table 1) were the same as in the experimental work.[1]

3. Results and Discussion

3.1. General Considerations

We have previously demonstrated experimentally that complex high-order (up to 20 blocks) multiblock copolymers with low dispersity can be prepared by one-pot RAFT polymerization based on sequential monomer addition by proper optimization of the polymerization conditions.[1,26] The key factor is to select conditions such that the polymerization rate is sufficiently high despite the initiator concentration being low, in combination with a sufficiently high ratio [RAFT agent]$_0$/[initiator]$_0$. Prior to our recent experimental work, it had been generally believed that the livingness inevitably decreases dramatically at high conversion. If this were the case, multiblock copolymer synthesis where each step is taken to full conversion would not be possible.

Table 1. Initial concentrations at the beginning of each cycle (for exact amounts of monomer, solvent and initiator added at the beginning of each cycle, see Supporting Information, Table S1 in ref.[1]).

Cycle	$[AIBN]_0$ [M]	$[DMA]_0$ [M]	$[macroRAFT]_0/[AIBN]_0$
2	1.400E − 03	1.51	108
3	1.140E − 03	1.2	105
4	9.530E − 04	0.99	104
5	8.140E − 04	0.85	104
6	7.100E − 04	0.74	104
7	6.290E − 04	0.65	104
8	5.650E − 04	0.59	104
9	5.120E − 04	0.53	104
10	4.690E − 04	0.49	104

The system modeled was the one-pot synthesis of a decamer (10 blocks) of poly(DMA) with an average degree of polymerization of 10 for each block ($[PDMA_{10}]_{10}$) in dioxane at 65 °C using PABTC as RAFT agent and AIBN as initiator, with a polymerization time of 24 h per block to ensure full conversion. Before each cycle, monomer, solvent, and initiator were added, resulting in initial concentrations for each cycle as detailed in Table 1. The experimental conditions modeled correspond to the experimental work reported earlier.[1]

Experimental conversion-time data are not available – in the experimental phase of this work,[1] the sole concern was that 100% conversion was reached over the polymerization time. The PREDICI simulations resulted in full conversion in <24 h for Cycles 2–10.

The livingness (L) in a RAFT polymerization (or any degenerative transfer system, assuming the living end groups (e.g., RAFT moiety) are not significantly consumed in side reactions, which is typically the case) is given by Equation 12:[1]

$$L = \frac{[\mathrm{RAFT}]_0}{[\mathrm{RAFT}]_0 + 2f[\mathrm{I}]_0(1 - e^{-k_d t})(1 - (f_c/2))} \quad (12)$$

where $[RAFT]_0$ and $[I]_0$ are the initial concentrations of RAFT agent and initiator, respectively, and f is the initiator efficiency (=0.5). The term $1 - f_c/2$ represents the number of chains produced in a radical–radical termination event with f_c the coupling factor ($f_c = 1$ means 100% bimolecular termination by combination, $f_c = 0$ means 100% bimolecular termination by disproportionation, as assumed in the present work). Importantly, Equation 12 correctly states that the livingness is solely dependent on the number of radicals generated from the initiator over the course of the polymerization – the instantaneous radical concentration is irrelevant (because all radicals generated via decomposition of the initiator will eventually terminate, before or after undergoing chain transfer events). Based on Equation 12, $L = 99.4\%$ is predicted for the polymerization of Cycle 1, which has the experimental values of $\overline{M}_n = 420\ \mathrm{g\ mol^{-1}}$ and $\overline{M}_w/\overline{M}_n = 1.18$ (i.e., this MWD was used as macroRAFT for the simulation of Cycle 2).

Figure 1 shows the entire set of full MWDs obtained by simulations of the iterative RAFT polymerizations corresponding to Cycles 2–10. The first observation is that excellent control over all MWDs is obtained; the MWDs shift to higher MWs with each successive Cycle, and there is

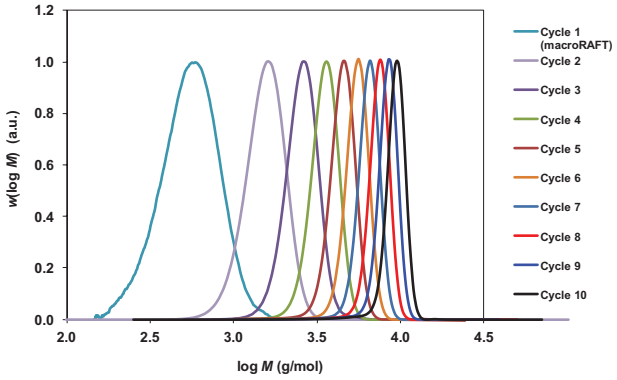

Figure 1. Simulations of iterative RAFT polymerizations corresponding to Cycles 2–10 (Cycle 1 corresponds to experimental MWD, which was employed as macroRAFT for Cycle 2). Dispersities: Cycle 1: 1.18; 2: 1.08; 3: 1.06; 4: 1.05; 5: 1.04; 6: 1.04; 7: 1.03; 8: 1.03; 9: 1.03; 10: 1.03.

minimal low MW tailing. As such, these simulations are overall in agreement with our recent experimental work, demonstrating that high order multiblock copolymers can be prepared by this approach.

Figure 2 shows overlays of the previously published[1] experimental MWDs and the simulated MWDs for Cycles 2, 6, and 10. A number of factors may account for the differences observed between the experimental and simulated MWDs. First of all, the experimental MWDs are not absolute – the MWs have been measured by size-exclusion chromatography (SEC) in DMF using linear polystyrene samples as standards. As discussed in our previous paper, it is likely that the use of polystyrene standards resulted in underestimation of the experimental MWs, which is consistent with the experimental MWDs (as well as the peak positions) being shifted to lower MWs than the simulated MWDs. One reason for the experimental MWDs being markedly broader than the simulated MWDs is SEC band broadening,[49] which has not been accounted for in the simulations. In our earlier paper,[1] we suggested that the low MW tailing seen in the experimental MWDs was partly caused by interactions between the polymer and the SEC column. This explanation is supported by the PREDICI simulations, which show that significant low MW tailing is not to be expected in the present system. However, it is of course also possible that imperfections in the model employed partly account for the narrow simulated MWDs. For example, the model does not account for any side reactions involving intermediate RAFT adduct radicals. The width of the MWD in LRP is closely associated with the number of activation/deactivation cycles an individual chain experiences as it grows to its final degree of polymerization[50]–the greater the number of such cycles, the narrower is the MWD. It is possible that the rate of exchange between active/dormant states is

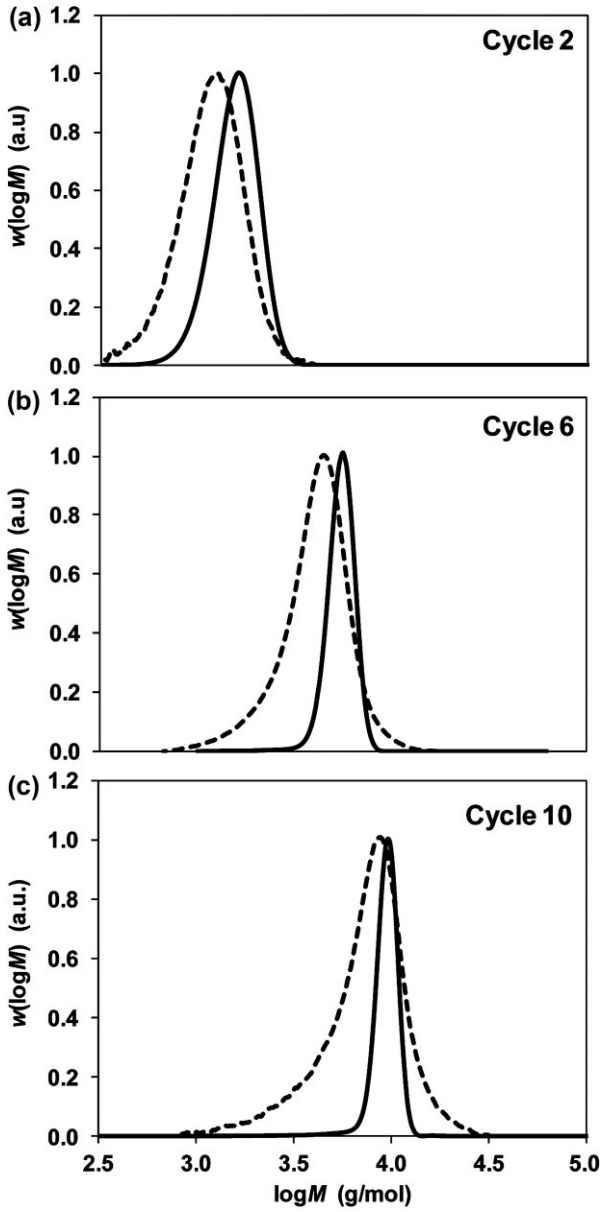

Figure 2. Experimental[1] (dotted lines) and simulated (full lines) MWDs of iterative RAFT polymerizations corresponding to Cycles 2 (a), 6 (b) and 10 (c).

overestimated in the model (i.e., the value of C_{ex} is too high). However, it is important to note that the value of C_{ex} does not influence the level of termination and the degree of livingness within the framework of the present model.

3.2. Livingness

Figure 3 shows the number fraction of dead polymer chains (relative to total number of chains) as a function of number of Cycles. The number of dead chains generated in Cycle 1

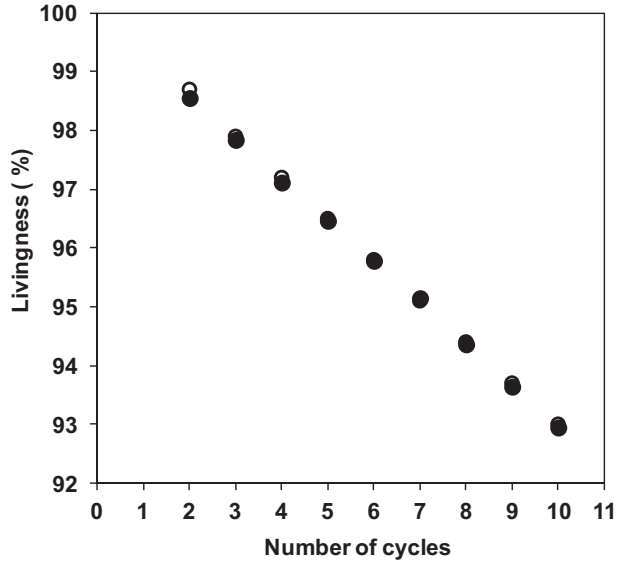

Figure 3. Livingness (percentage by number of chains with RAFT moiety as ω-end group) as a function of the number of cycles for iterative RAFT polymerization as predicted by simulations (●) and by use of Equation 12 (○).

(0.6% based on Equation 12; not accounted for in the simulations since the final MWD of Cycle 1 was treated as macroRAFT for Cycle 2–see above) was corrected for when plotting the livingness for the simulated data. The numbers of dead chains obtained by the PREDICI simulations are in near perfect agreement with the number of chains generated from the initiator, as expected, in agreement with Equation 12. The very minor disagreement seen for Cycle 2 in particular can be attributed to numerical error associated with the simulations. It is important to note that Equation 12 was not used in any way in connection with the PREDICI simulations. The agreement between simulations and Equation 12 confirms that the livingness is solely governed by the number of chains generated from the initiator (i.e., the number of new chains) relative to the initial number of macroRAFT. This may seem obvious. However, examination of the vast literature on RAFT polymerization reveals that it is only too common to find statements alluding to the fact that the propagating radical concentration as well as high conversion have detrimental effects on livingness. This is incorrect – all that matters is the number of new chains generated by the initiator during the course of the polymerization relative to the number of chains with RAFT end groups (i.e., initial RAFT agent). Moreover, this is true for all degenerative transfer LRP system, and it is exploitation of this fundamental feature that has enabled us to develop methodology for synthesis of high order multiblock copolymers by RAFT polymerization.[1,26] At the end of Cycle 10, the simulations (and Equation 12) predict ≈7% dead chains by number.

The number-average MW (number of monomer units reacted divided by number of chains) is typically plotted versus conversion to evaluate the controlled/living characteristics of a LRP process. In the present case, such a plot is redundant given that the data in Figure 2 already demonstrate that the number of chains in the simulations is given by the denominator of Equation 12.

3.3. MWDs of Living and Dead Chains

Figure 4a shows simulated MWDs normalized to peak height corresponding to living and dead chains after Cycle 2. These data provide information on where in the overall MWD the dead chains appear. The two MWDs are in fact very similar, with the MWD corresponding to the dead chains being shifted slightly to lower MWs. The reason for this shift is that chains terminate "prematurely," and as such their growth is interrupted (note that termination occurs by disproportionation only). Figure 4b shows the living and dead MWDs after Cycle 3. The dead MWD is now significantly broader, which has its origin in there being two "crops" of dead chains (clearly visible in the MWD), corresponding to those formed during Cycles 2 and 3. The MWD of the dead chains after Cycle 4 is further broadened (Figure 4c), displaying the clear characteristics of three "crops." A low MW tail is gradually formed as the number of Cycles increases, because dead polymer chains are inevitably "left behind" – the exact number of such chains corresponds to the number of radicals generated from the radical initiator during the polymerization time of each Cycle, i.e., there are more chains in the system than there are RAFT end groups. In addition to low MW shoulders being generated by chains undergoing termination, new chains are of course also generated continuously by the initiator, thus adding to the low MW tail (see further discussion below).

The contribution of the dead chains to the overall MWDs in Cycles 2–4 is vanishingly small (MWDs in Figure 4 have been normalized to peak height), as evident from the fact that the number fraction of dead chains after Cycle 4 is $<3\%$ (Figure 3). This point is further illustrated in Figure 5a, which quantitatively shows the final dead and living MWDs after Cycle 10. There is a significant low MW tail in the dead MWD (Figure 5b), however, this tail is barely visible in the overall MWD (Figure 1) because of the low number fraction of dead chains (≈7% after Cycle 10; Figure 3). Figure 6 shows quantitative MWDs of the dead and living chains after Cycle 10 in the form of number distributions (i.e., y-axis is proportional to number of chains N, as opposed to NM^2 (M = molecular weight) in the "GPC distributions" ($w(\log M)$). This representation of the MWDs puts more emphasis on any low MW tail that may be present. The zoomed in plot in Figure 6b reveals that there is a low MW tail of dead chains that decreases in intensity

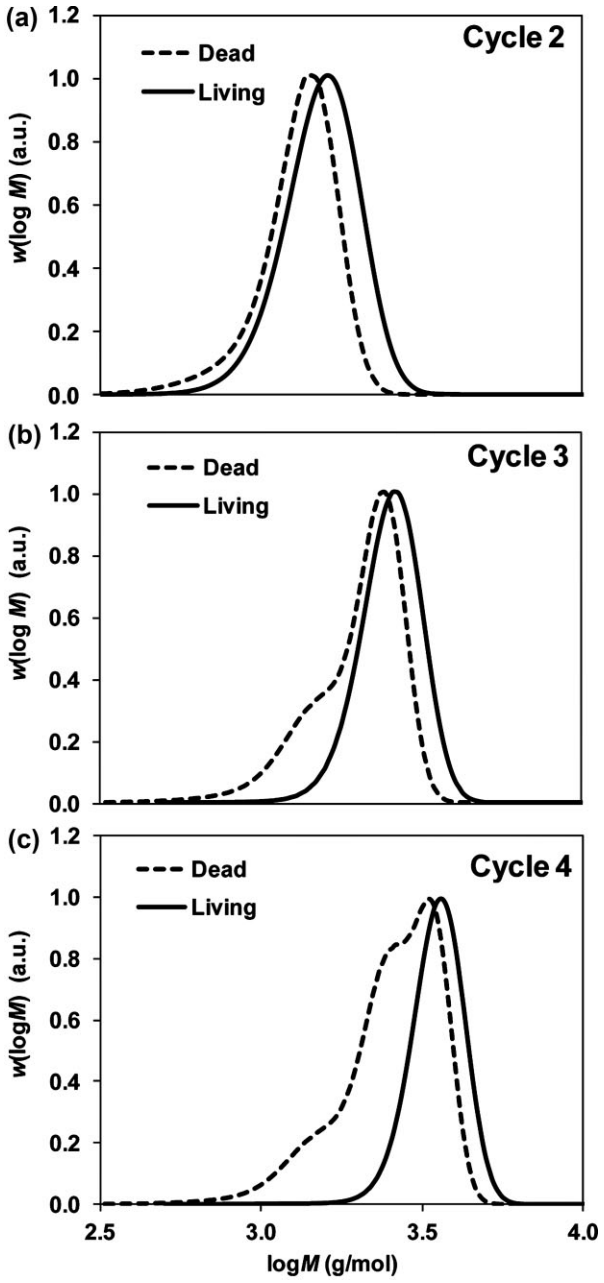

Figure 4. MWDs (normalized to peak height) corresponding to living (chains with RAFT moiety as ω-end group) and dead chains for iterative RAFT polymerizations simulated using PREDICI for Cycles 2 (a), 3 (b), and 4 (c).

with decreasing MW, consistent with the data displayed in Figure 4. The number distribution reveals that there is also a low MW tail in the living MWD – this low MW tail has its origin in the fact that short chains are continuously generated via decomposition of the initiator, and these short chains may be converted to living chains via chain transfer with a RAFT moiety, or dead chains via termination.

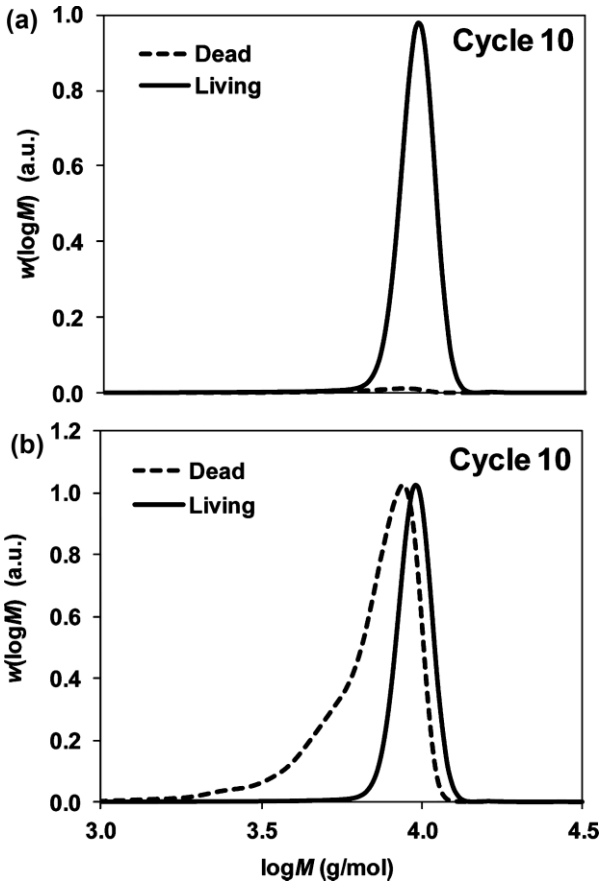

Figure 5. Quantitative MWDs (a) and MWDs normalized to peak height (b) for living (chains with RAFT moiety as ω-end group) and dead chains for iterative RAFT polymerizations simulated using PREDICI after Cycle 10.

4. Conclusions

Modeling and simulations have been conducted using the software PREDICI to examine the recently reported[1,26] one-pot sequential monomer addition RAFT polymerization approach toward well-defined high order multiblock copolymers. The system modeled is the iterative homopolymerizations (10 cycles) of DMA in dioxane at 65 °C using PABTC as RAFT agent and AIBN as initiator, which we have recently studied experimentally.[1]

It is confirmed that RAFT polymerization (in fact, degenerative transfer systems in general) is well suited for synthesis of high-order multiblock copolymers by sequential monomer addition, where each step is taken to near full monomer conversion without intermediate purification. The key to success is the realization that the number fraction of dead chains is accurately known from the number of chains generated from the radical initiator, and as such conditions can be tailored with regards to the level of livingness required. In the present case, despite as

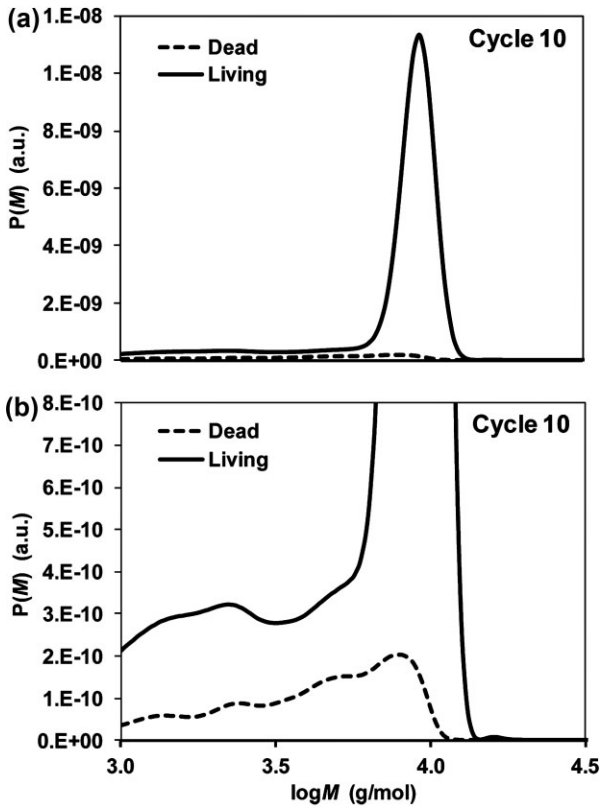

Figure 6. Quantitative MWDs by number (number distributions) for living (chains with RAFT moiety as ω-end group) and dead chains for iterative RAFT polymerizations simulated using PREDICI after Cycle 10; in (b), the y-axis has been scaled to increase visibility of low MW tails (no such scaling in (a)).

many as 10 iterative RAFT polymerization steps to full monomer conversion, the number fraction of dead chains at the end of Cycle 10 is only ≈7%.

These results further demonstrate the future potential of LRP systems based on degenerative transfer (most notably RAFT) for synthesis of sequence-controlled copolymers.

Received: November 27, 2013; Published online: February 20, 2014; DOI: 10.1002/mats.201300165

Keywords: multiblock copolymers; RAFT polymerization; PREDICI

[1] G. Gody, T. Maschmeyer, P. B. Zetterlund, S. Perrier, *Macromolecules* **2014**, *47*, 639.
[2] N. Badi, D. Chan-Seng, J. F. Lutz, *Macromol. Chem. Phys.* **2013**, *214*, 135.
[3] J.-F. Lutz, M. Ouchi, D. R. Liu, M. Sawamoto, *Science* **2013**, *341*, 1238149.
[4] M. Ouchi, N. Badi, J. F. Lutz, M. Sawamoto, *Nat. Chem.* **2011**, *3*, 917.
[5] A. M. Rosales, R. A. Segalman, R. N. Zuckermann, *Soft Matter* **2013**, *9*, 8400.
[6] W. A. Braunecker, K. Matyjaszewski, *Prog. Polym. Sci.* **2007**, *32*, 93.
[7] P. B. Zetterlund, Y. Kagawa, M. Okubo, *Chem. Rev.* **2008**, *108*, 3747.
[8] Y. Hibi, M. Ouchi, M. Sawamoto, *Angew. Chem. Int. Ed.* **2011**, *50*, 7434.
[9] S. Ida, M. Ouchi, M. Sawamoto, *Macromol. Rapid Commun.* **2011**, *32*, 209.
[10] B. Schmidt, N. Fechler, J. Falkenhagen, J. F. Lutz, *Nat. Chem.* **2011**, *3*, 234.
[11] X. M. Tong, B. H. Guo, Y. B. Huang, *Chem. Commun.* **2011**, *47*, 1455.
[12] J. Niu, R. Hili, D. R. Liu, *Nat. Chem.* **2013**, *5*, 282.
[13] R. McHale, J. P. Patterson, P. B. Zetterlund, R. K. O'Reilly, *Nat. Chem.* **2012**, *4*, 491.
[14] F. S. Bates, M. A. Hillmyer, T. P. Lodge, C. M. Bates, K. T. Delaney, G. H. Fredrickson, *Science* **2012**, *336*, 434.
[15] M. Mertoglu, S. Garnier, A. Laschewsky, K. Skrabania, J. Storsberg, *Polymer* **2005**, *46*, 7726.
[16] Y. K. Huang, T. T. Hou, X. Q. Cao, S. Perrier, Y. L. Zhao, *Polym. Chem.* **2010**, *1*, 1615.
[17] J. Vandenbergh, T. D. Ogawa, T. Junkers, *J. Polym. Sci. A: Polym. Chem.* **2013**, *51*, 2366.
[18] N. A. Hadjiantoniou, A. I. Triftaridou, D. Kafouris, M. Gradzielski, C. S. Patrickios, *Macromolecules* **2009**, *42*, 5492.
[19] F. Nystrom, A. H. Soeriyadi, C. Boyer, P. B. Zetterlund, M. R. Whittaker, *J. Polym. Sci. A: Polym. Chem.* **2011**, *49*, 5313.
[20] C. Boyer, A. H. Soeriyadi, P. B. Zetterlund, M. R. Whittaker, *Macromolecules* **2011**, *44*, 8028.
[21] A. H. Soeriyadi, C. Boyer, F. Nystrom, P. B. Zetterlund, M. R. Whittaker, *J. Am. Chem. Soc.* **2011**, *133*, 11128.
[22] C. Boyer, A. Derveaux, P. B. Zetterlund, M. R. Whittaker, *Polym. Chem.* **2012**, *3*, 117.
[23] A. Anastasakia, C. Waldron, P. Wilson, C. Boyer, P. B. Zetterlund, M. R. Whittaker, D. Haddleton, *ACS Macro Lett.* **2013**, *2*, 896.
[24] Q. Zhang, P. Wilson, Z. D. Li, R. McHale, J. Godfrey, A. Anastasaki, C. Waldron, D. M. Haddleton, *J. Am. Chem. Soc.* **2013**, *135*, 7355.
[25] Q. Zhang, J. Collins, A. Anastasaki, R. Wallis, D. A. Mitchell, C. R. Becer, D. M. Haddleton, *Angew. Chem. Int. Ed.* **2013**, *52*, 4435.
[26] G. Gody, T. Maschmeyer, P. B. Zetterlund, S. Perrier, *Nat. Commun.* **2013**, *4*, 2505.
[27] M. Wulkow, *Macromol. React. Eng.* **2008**, *2*, 461.
[28] C. Barner-Kowollik, M. Buback, B. Charleux, M. L. Coote, M. Drache, T. Fukuda, A. Goto, B. Klumperman, A. B. Lowe, J. B. McLeary, G. Moad, M. J. Monteiro, R. D. Sanderson, M. P. Tonge, P. Vana, *J. Polym. Sci. A: Polym. Chem.* **2006**, *44*, 5809.
[29] J. Chiefari, Y. K. Chong, F. Ercole, J. Krstina, J. Jeffery, T. P. T. Le, R. T. A. Mayadunne, G. F. Meijs, C. L. Moad, G. Moad, E. Rizzardo, S. H. Thang, *Macromolecules* **1998**, *31*, 5559.
[30] S. Perrier, P. Takolpuckdee, *J. Polym. Sci. A: Polym. Chem.* **2005**, *43*, 5347.
[31] C. Barner-Kowollik, S. Perrier, *J. Polym. Sci. A: Polym. Chem.* **2008**, *46*, 5715.
[32] G. Moad, E. Rizzardo, S. H. Thang, *Aust. J. Chem.* **2012**, *65*, 985.
[33] D. Konkolewicz, B. S. Hawkett, A. Gray-Weale, S. Perrier, *Macromolecules* **2008**, *41*, 6400.
[34] D. Konkolewicz, B. S. Hawkett, A. Gray-Weale, S. Perrier, *J. Polym. Sci. A: Polym. Chem.* **2009**, *47*, 3455.

[35] S. R. S. Ting, T. P. Davis, P. B. Zetterlund, *Macromolecules* **2011**, *44*, 4187.
[36] T. Junkers, G. Delaittre, R. Chapman, F. Gunzler, E. Chernikova, C. Barner-Kowollik, *Macromol. Rapid Commun.* **2012**, *33*, 984.
[37] W. Meiser, M. Buback, *Macromol. Rapid Commun.* **2012**, *33*, 1273.
[38] P. B. Zetterlund, K. Miyake, K. Goto, B. Yamada, *J. Polym. Sci. A: Polym. Chem.* **2004**, *42*, 2640.
[39] M. Wulkow, M. Busch, T. P. Davis, C. Barner-Kowollik, *J. Polym. Sci. A: Polym. Chem.* **2004**, *42*, 1441.
[40] P. B. Zetterlund, S. Perrier, *Macromolecules* **2011**, *44*, 1340.
[41] S. A. Seabrook, M. P. Tonge, R. G. Gilbert, *J. Polym. Sci. A: Polym. Chem.* **2005**, *43*, 1357.
[42] F. Ganachaud, M. J. Monteiro, R. G. Gilbert, *Macromol. Symp.* **2000**, *150*, 275.
[43] K. W. Dixon, in *Polymer Handbook*, (Eds., J. Brandrup, E. H. Immergut, E. A. Grulke), Wiley, New York **1999**, p. II/12.
[44] M. Destarac, *Polym. Rev.* **2011**, *51*, 163.
[45] D. Konkolewicz, M. Siauw, A. Gray-Weale, B. S. Hawkett, S. Perrier, *J. Phys. Chem. B* **2009**, *113*, 7086.
[46] G. B. Smith, G. T. Russell, J. P. A. Heuts, *Macromol. Theory Simul.* **2003**, *12*, 299.
[47] C. Barner-Kowollik, G. T. Russell, *Prog. Polym. Sci.* **2009**, *34*, 1211.
[48] T. Junkers, A. Theis, M. Buback, T. P. Davis, M. H. Stenzel, P. Vana, C. Barner-Kowollik, *Macromolecules* **2005**, *38*, 9497.
[49] J. V. Castro, K. Y. van Berkel, G. T. Russell, R. G. Gilbert, *Aust. J. Chem.* **2005**, *58*, 178.
[50] A. Goto, T. Fukuda, *Prog. Polym. Sci.* **2004**, *29*, 329.